euspen's 23rd International Conference & Exhibition, Copenhagen, DK, June 2023
www.euspen.eu

Miniature flexure-based goniometer with minimized parasitic motion

Elwin Vree[1], Hendrik-Marten Meyer[2], and Jan de Jong[1]

[1]*Precision Engineering Lab, University of Twente, Enschede, The Netherlands*
[2]*SmarAct GmbH, Oldenburg, Germany*

j.j.dejong@utwente.nl

Abstract
Precise positioning systems often rely on flexure-based mechanisms. Since flexures move by elastic deformation, they feature zero wear, virtually no hysteresis and potentially higher motion repeatability when compared to conventional bearings. This renders them especially suited for precision applications and for special environments such as ultra-high vacuum. However, limited stroke, load-capacity and nonlinear geometric behavior over the stroke, termed parasitic motion, make the design of such mechanisms challenging. Therefore, the rotation of existing flexure-based goniometers is restricted to small angles. In this paper, we demonstrate a small-scale goniometer based on a flexure guiding system with low parasitic motion over several degree of rotational motion. By stacking six trapezoidal flexure stages with an alternating orientation, the parasitic motion of the 'face-up' stages is counteracted by the 'face-down' stages leading to a significant reduction of parasitic motion. This butterfly-like structure also reduces the deformation per flexure, allowing for a higher thickness with improved loadability and support stiffness. The final prototype has a range of ± 3 deg, a repeatability of 70 μdeg and a parasitic motion of 5.0 μm under a payload of 100 g.

Keywords: Flexure-based, Goniometer, Parasitic motion

1. Introduction

Precise positioning using contact-based bearings can lead to known issues like friction, wear and require lubricant which makes applications in special environments like ultra-high vacuum or ultra-low temperatures challenging. Flexure-based bearings allow motion by bending, leading to high predictability and motion precision [1]. However, the kinematics of flexures change nonlinearly over deflection, leading to repeatable but unwanted parasitic motion. Furthermore, stress build-up and increased actuator load limits the flexures' thickness, leading to limited support stiffness and stroke. This makes designing flexure-hinges challenging, especially for small-scale applications were manufacturing and assembly tolerances are tight.

In search of a highly precise small-scale goniometer, we investigate if a flexure-based hinge may result in improved position precision. Goniometers are used in precision applications to rotate for example a specimen in a microscope [2] or a mirror in telescope about a remote pivot point. Other applications include spectroscopy and high energy research [3].

In these applications it is essential that the pivot point is well defined and the intrinsic parasitic motion of the flexure hinge is minimal, even under relatively high loads. Literature shows that parasitic motion may be reduced by selecting specific dimensions [4] or by adding compensating structures [5], termed compounding [6].

In this paper we propose a small-scale, large-stroke flexure-based goniometer that employs multiple parasitic motion compensating stages as a viable alternative to contact-based bearing goniometers. We particularly show that parasitic motion is composed of a kinematically-induced and load-induced part, which, by selection of actuator strategy, are designed to partially negate each other. We furthermore investigate the effectiveness of increasing the number of parasitic motion compensation stages.

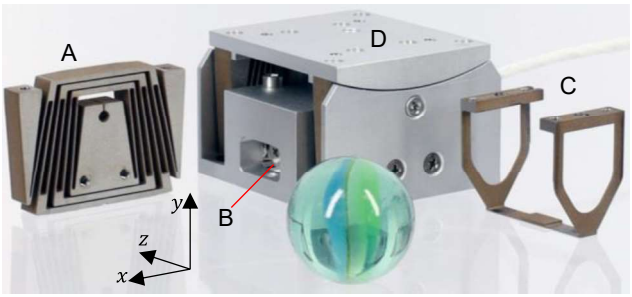

Figure 1. The small-scale goniometer consists of two stacks of triply compounded flexure hinges (A) to minimize parasitic motion ($\lesssim$ 10 µm) and retain a high-support stiffness over the range of motion. It is driven by a SmarAct piezo stepper (B) that is connected via a double folded leaf spring (C) to the top plate (D). A marble (Ø 16 mm) is shown for scale.

The paper is organized as followed: first we discuss the design and the design process after that we show effects of three design choices and we end with a repeatability and accuracy validation of the prototype.

2. Design

2.1 Requirements and scope

The goniometer is designed to perform a repeatable rotation of $\pm$ 3 deg about a pivot point 35 mm above the top plate. To have a well-defined pivot point, the parasitic motion under deflection should be small. To increase its potential range of applications, it should be made from ultra-high vacuum compatible and non-magnetic components and feature a small building space. To eventually fit in small cryo and vacuum chambers, its footprint should remain small leading to potential

Table 1. List of requirements for small scale goniometer

	Requirement		Value	Unit
1	Range of motion (±)	≥	3.0	deg
2	Pivot distance	=	35	mm
3	Parasitic motion	≤	10	µm
4	Repeatability	≤	100	µdeg
5	Load capacity	≥	100	g
6	Actuation force	≤	1.0	N
7	Flexure thickness	≥	0.15	mm
8	Build volume (x, y, z)	≤	$30 \times 20 \times 30$	mm^3

manufacturing and assembly constraints. At this scale especially the minimal thickness of wire erosion is challenging. The actuation stiffness of the mechanisms should be limited to prevent overloading of small-scale piezo steppers. The full list of requirements can be found in Table 1.

2.2 Topology and design process

The designed goniometer (Figure 1) consist of a flexure-based hinge with a virtual pivot point that is driven by a linear piezo stepper with a conventional bearing and integrated encoder.

To make best possible use of the build volume, the hinge consists of two stacks of multiple-compounded leaf springs on each side of the actuator. Folded leaf springs connect the actuator to the top-plate to solely transmit the actuation force and decouple the other motion directions.

The design parameters are chosen through a model-based optimization routine that minimizes the parasitic motion while adhering to the set requirements and avoid collision during motion. The optimized parameters are the number of stages, the width, and the thickness of the flexures. The maximal available flexures' length chosen. This optimization uses a flexible multibody program [7] to model the flexures' non-linear behavior. All evaluations were done at a the maximum payload.

2.3 Minimizing parasitic motion

To justify the final design, we evaluate the effects of different design parameters while only changing one design parameter at a time. Here we report the effects of changing 1) the type of actuation, 2) the number of stages and 3) the payload.

1) The proposed goniometer is actuated by a linear motor at a distance to produce the required actuation moment. It may be expected that this force in combination with limited support stiffness induce additional parasitic motion when compared to a pure moment. Furthermore, the folded leaf spring may induce an actuation stiffness that may influence the parasitic motion. We therefore evaluate the parasitic motion in x- and y-direction for three actuation types: pure moment, force at a distance and displacement of a folded leaf spring (actual realization).

2) A key feature in this design is the use of a compounded flexure hinge with many intermediate stages. We will evaluate the effect of the number of stages on the parasitic motion. To make a valid comparison, we reduce the width w of the flexures to stay within the same actuation limit of $1\ N$.

3) To make a distinction between kinematically induced and load induced parasitic motion we evaluate 0, 50 and 100 g payloads.

2.4 Validation method

The constructed goniometer is validated for linearity, repeatability, and parasitic motion by measuring the displacement and rotation of the top-plate with a dual channel interferometer and two retroreflectors that are placed on the top-plate.

In the linearity and repeatability test, the measured angle of the top plate is compared to the translation of the actuator as measured by its integrated linear encoder. In the range of motion, 20 poses are evaluated over 10 motion cycles.

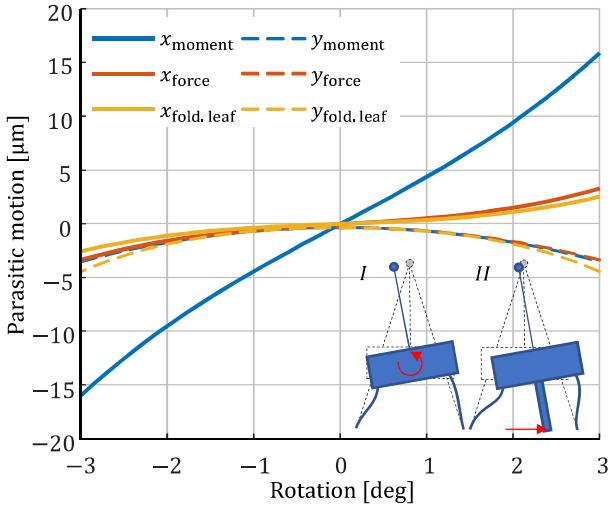

Figure 2. The simulated parasitic motion in the x- and y-direction when actuated by a pure moment, a pure force at the linear actuator location and the displacement of the set of folded leaf springs. The inserts illustrate how the moment actuated hinge (***I***) experiences more parasitic motion then the force actuated hinge (***II***).

For the parasitic motion test, we additionally estimate the displacement in the direction of the interferometer beam. Since we are interested the x and y displacement under rotation, we perform a top and a side view measurement. Due to limitations of the current set-up, it is not possible to compute the absolute parasitic motion as the location of the retroreflectors with respect to the intended pivot point is not known in both measurements. The mass of the retro-reflectors setup is 42 g.

3. Results

3.1 Parasitic motion minimization

3.1.1 Actuation type

When actuated by a pure moment, the goniometer shows a significant parasitic motion in the x-direction due to shortening of the flexure (Figure 2). In the vertical direction the system moves down while in the horizontal direction it moves in negative direction.

When actuating with a force at the intended point of the actuator, a part of the parasitic movement in the x-direction is compensated by static deflection caused by the actuation force, improving the parasitic motion significantly. In the vertical direction, no significant changes are observed.

Since we use piezo stepper motors with a rectilinear motion, we decouple the rotation by using two folded leaf springs. This results in a marginal change of the parasitic motion due to additional stiffness in the actuation direction.

These results clearly indicate that parasitic motion is not a purely kinematic effect but is also influenced by the static loading of the system.

It may be inferred that a load application point closer to the virtual pivot point would result in more actuation force and more parasitic motion compensation. However, this would also exceed the available actuator force.

From the graphs it may be observed that the parasitic motion in the x-direction is characterized by a 1st and a 3rd order effect, while in the y-direction it is dominated by quadratic effects.

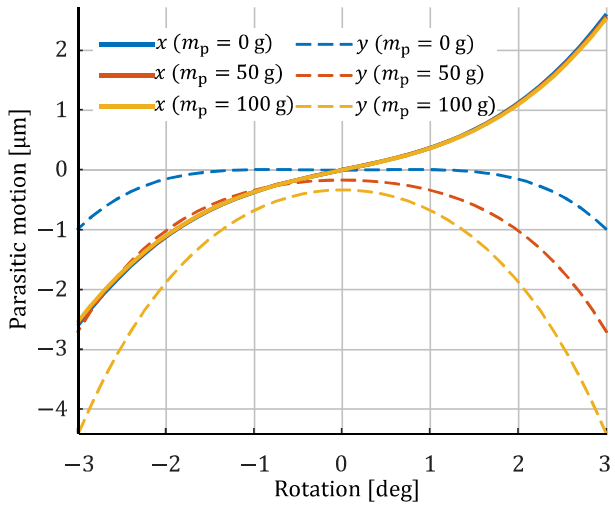

Figure 3. The simulated parasitic motion in $\boldsymbol{x}$ (horizontal) and $\boldsymbol{y}$ (vertical) direction of a triple stage layout for various payloads $\boldsymbol{m_p}$.

3.1.2 Payload

Simulations show that a larger payload increases the parasitic motion in the vertical direction, while the horizontal direction is hardly affected (Figure 3).

In the neutral position a little sag is observed, while the vertical sag becomes larger at deflection. This indicates that a significant portion of the parasitic motion in the vertical direction is due to elastic effects, i.e., due to the reduced stiffness of the flexures at deflection. This indicates that lowering the payload may reduce the parasitic motion significantly.

3.1.3 Number of stages

The simulation results show that increasing the number of stages reduces parasitic motion (Figure 4). In fact, it follows a quadratic trend with the number of stacks.

Partly, this can be explained by the fact that motion is distributed over multiple stages which, due to their non-linear behavior, reduce the total parasitic motion. As seen in Figure 2 the parasitic motion in the x-direction has the shape of

$$p_{e,x} \approx \alpha n(\phi/n) + \gamma n(\phi/n)^3 = \alpha\phi + \frac{\gamma}{n^2}\phi^3, \qquad (1)$$

where n is the number of stages, ϕ is the deflection angle, and α and γ are unknown constants. This implies that, if α is sufficiently small, the parasitic motion decreases quadratically with the number of stages.

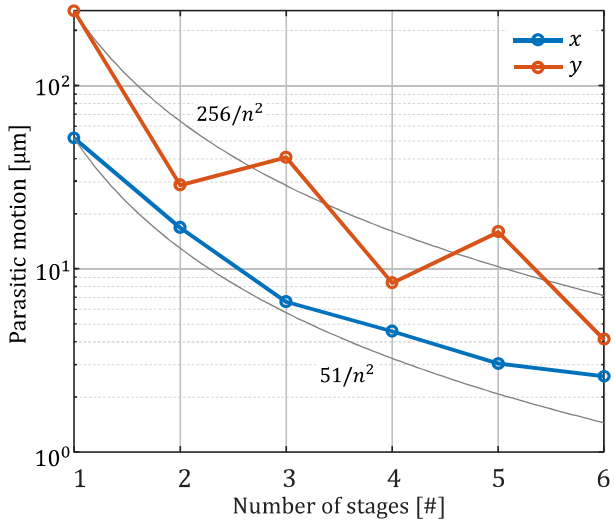

Figure 4. The simulated parasitic motion in x- and y-direction at full deflection for different number of stages. Two trendlines indicate the inverse quadratic effect on the number of stages $\boldsymbol{n}$.

For the y-direction such an explanation is not satisfactory as the parasitic motion is quadratic in the angle and we would therefore expect a linear relation between the number of stages and the parasitic motion. Here another effect comes in to play, that is, the reduced actuation stiffness for higher number of stages ($f_{act} \propto w/n$) allow for wider leaf springs with more support stiffness ($k_{yy} \propto w$) under deflection and thus less parasitic effects ($P_{e,y} \propto \phi^2/n^2$) due to the payload, here the width is denoted with w.

An even number of stages performs better as positively oriented stages compensate the y-parasitic motion of a negatively oriented stage. This shortening compensation is used in the double parallel leaf spring mechanism [8] and the butterfly hinge [6].

A further increase of the number of stages would reduce the parasitic motion further. However, the relative gain is reduced and more than 6 stages would run in to practical limitations.

3.2 Validation

3.2.1 Linearity and repeatability

Interferometric measurements show that the top-plate angle is highly linear with the actuation of the motor (Figure 5 top). Moreover, it shows that the remaining non-linearity has the same shape and is of the same order as the simulation results (Figure 5 bottom). This indicates that this non-linearity can be calibrated and compensated for, allowing a well controllable motion.

Compared to simulation, actual system shows a slightly smaller rotation angle at the same actuator. This is potentially due to higher compliance in drive train, e.g., non-rigidity of the frame parts.

By visiting the same actuation point multiple times, the repeatability of the system can be estimated. Figure 5 bottom we show the bidirectional repeatability (σ_b) is about 70 µdeg, whereas the unidirection repeatability is about 35 µdeg.

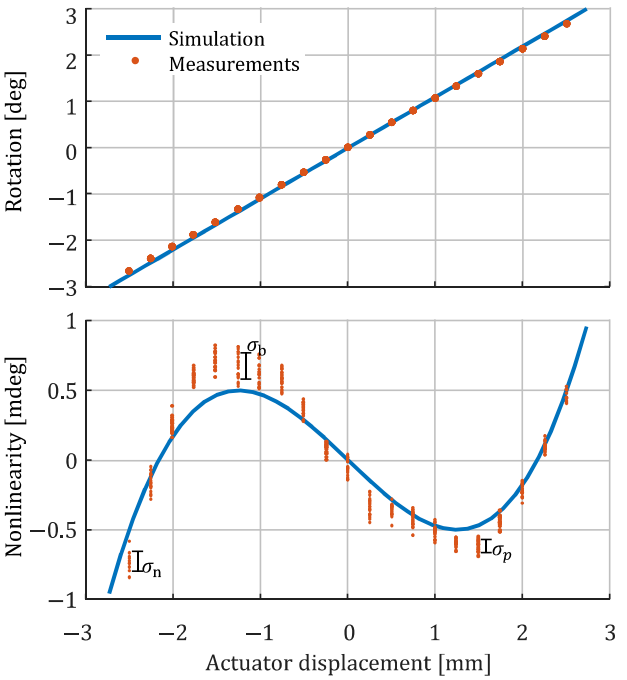

Figure 5. (top) Measurements and simulations of the rotation of the top-plate for various actuator positions. **(bottom)** Residual of a linear fit through measured rotation angle shows a clear trend with simulation. The maximum variation for positive ($\boldsymbol{\sigma_p}$), negative ($\boldsymbol{\sigma_n}$), and bidirectional ($\boldsymbol{\sigma_b}$) motion is indicated by error bars.

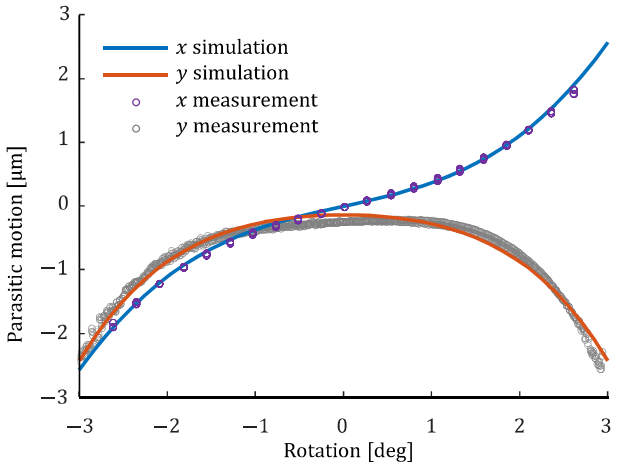

Figure 6. The simulated and measured parasitic motion in x (horizontal) and y (vertical) direction.

This is close to the repeatability that can be expected from the linear actuator, indicating that the flexure stage does not induce significant hysteresis effects.

3.2.2 Parasitic motion

By measuring the translation and rotation of the top-plate with an interferometer an estimate for the x and y translation over rotation angle could be made. From this, the parasitic motion in both directions may be estimated.

Since we use a dual head interferometer, we could only identify the parasitic motion in one direction at the time. Additionally, since the retroreflectors could not be accurately aligned with the top plate, the parasitic motion estimation is obtained by fitting the measurement to the simulation. The parasitic motion is therefore not the absolute displacement of the initial pivot, but of a point that explains the measurements the best. Linear and quadratic effects have been compensated for by shifting this evaluation point.

These measurements indicate that the parasitic motion is highly repeatable. Additionally, it shows that the cubic effects in the x-direction are in the same order as the simulation. The quartic effects in the y-direction seem slightly larger than in simulation, possibly indicating more parasitic effects in this direction.

4. Conclusion

A flexure-based goniometer with ± 3 deg rotation around a remote pivot point is presented. Owing to its flexure-based design a bidirectional repeatability about 70 µdeg was achieved. Simulations showed that parasitic motion depend on both kinematic (shortening) and elastic (loading) effects. The parasitic motion was reduced by a factor of 55 by using 6 stages in alternate orientation. This way the parasitic motion of the up-facing stages is compensated by down-facing stages. Additionally, as the parasitic motion is a non-linear effect in the rotation angle, reducing the rotation of the individual stages lead to a reduction of the total parasitic motion. Furthermore, as the required actuation force reduces with the number of stages, wider flexures with more support stiffness may be used, reducing the load-dependent parasitic motion. In this design the actuation force compensates a part of the parasitic motion due to rotation. This leads to a theoretical parasitic motion of 5.0 μm under full load. Our results show that flexure-based hinges might provide a viable alternative in applications where conventional bearings are undesired.

References

[1] S. T. Smith, *Flexures: Elements of Elastic Mechanisms*. Taylor & Francis, 2000.

[2] W. Guan, A. Lockwood, B. J. Inkson, and G. Möbus, "A piezoelectric goniometer inside a transmission electron microscope goniometer," *Microsc. Microanal.*, vol. 17, no. 5, pp. 827–833, 2011, doi: 10.1017/S143192761100050X.

[3] M. Butcher, A. Giustiniani, R. Losito, and A. Masi, "Controller design and verification for a rotational piezo-based actuator for accurate positioning applications in noisy environments," *IECON 2015 - 41st Annu. Conf. IEEE Ind. Electron. Soc.*, pp. 3887–3892, 2015, doi: 10.1109/IECON.2015.7392706.

[4] Z. Hongzhe and B. Shusheng, "Accuracy characteristics of the generalized cross-spring pivot," *Mech. Mach. Theory*, vol. 45, no. 10, pp. 1434–1448, 2010, doi: 10.1016/j.mechmachtheory.2010.05.004.

[5] G. Hao, Q. Meng, and Y. Li, "Design of large-range XY compliant parallel manipulators based on parasitic motion compensation," *Proc. ASME Des. Eng. Tech. Conf.*, vol. 6 A, no. August, 2013, doi: 10.1115/DETC2013-12206.

[6] S. Henein, P. Spanoudakis, S. Droz, L. I. Myklebust, and E. Onillon, "Flexure pivot for aerospace mechanisms," *Eur. Sp. Agency, (Special Publ. ESA SP*, no. 524, pp. 285–288, 2003.

[7] J. Jonker and J. Meijaard, "SPACAR—Computer program for dynamic analysis of flexible spatial mechanisms and manipulators," in *Multibody systems handbook*, Springer, 1990, pp. 123–143.

[8] R. V. Jones, "Some uses of elasticity in instrument design," *J. Sci. Instrum.*, vol. 39, no. 5, pp. 193–203, 1962, doi: 10.1088/0950-7671/39/5/303.